

Remarks on a stochastic geometric model for interference-limited cellular communications

Hamed Nassar¹, Gehad Mohamed Taher¹, El Sayed El Hady^{2,3}

¹Department of Computer Science, Suez Canal University, Ismailia, Egypt

²Department of Basic Sciences, Suez Canal University, Ismailia, Egypt

³Department of Mathematics, College of Science, Jouf University, Al-Jawf, Saudi Arabia

Article Info

Article history:

Received Nov 18, 2023

Revised Jan 14, 2024

Accepted Jan 16, 2024

Keywords:

Base station density
Cellular communications
Coverage probability
IoT deployment
Stochastic geometry
Transmit power

ABSTRACT

A plethora of stochastic geometry (SG) models have been developed for cellular communications, especially in the context of internet of things (IoT) applications. A typical assumption in such models is that base stations (BS) are deployed in the Euclidean plane as a spatial poisson point process (PPP) of some density λ , with each communicating equipment transmitting at some power p . The usual objective of these models is to characterize the cellular coverage probability in both the downlink (DL) and uplink (UL) directions. In this article we expose, in the form of four remarks, the peculiar behavior of a baseline stochastic geometric model of an interference-limited cellular system. Specifically, we reveal that under some assumptions, the coverage probability in both the UL and DL directions for this system is independent of both λ and p , flagrantly contradicting intuition. The aim of the article is by no means to invalidate the use of SG in modeling communications systems, but rather to point out that such modeling may not be adequate all the time.

This is an open access article under the [CC BY-SA](https://creativecommons.org/licenses/by-sa/4.0/) license.



Corresponding Author:

Gehad Mohamed Taher
Department of Basic Sciences, Suez Canal University
Ismailia, Egypt
Email: gehad.taher@ci.suez.edu.eg

1. INTRODUCTION

Stochastic geometry (SG) has been used heavily as a modeling tool in the field of wireless communications, e.g., ad hoc networks, cellular networks and IoT device deployment. For example, SG has been used in [1] to model heterogeneous cellular networks, in [2] to model narrow band internet of things (IoT), in [3] to model D2D communications underlying cellular systems, and in [4] to model millimeter wave dense cellular networks. The SG model is based on treating the nodes as a realization (snapshot) of a spatial point process in the Euclidean plane, then averaging over all node locations to obtain useful performance metrics. The most common such metric is the signal to interference and noise ratio (SINR), which can then be used to calculate other useful metrics, such as coverage probability, network throughput and spectral efficiency, in both the downlink (DL) and uplink (UL) directions. However, it is interesting to note that with the explosive growth of wireless emissions in recent years, the impact of interference has largely outweighed noise [5] which has called for characterizing signal-to-interference (SIR) rather than SINR (see, for example, [6]-[8]), effectively adopting the interference limited assumption which is adopted also in the present article.

When using SG to model cellular networks, base stations (BS) are usually deployed in the Euclidean plane as a poisson point process (PPP), with some density λ . In this way, countless models have been developed for different wireless scenarios. Most of those models stress that coverage probability, in both the DL and UL directions, is dependent on both BS density λ and transmit power p , which seems intuitive enough. Examples of such models for DL can be found in [5], [6], [8]-[21]. On the other hand, examples of such models for UL can be found in [5], [7], [9], [16]-[25]. However, as we will show in this article, we can construct a cellular network scenario whereby the coverage probability, when evaluated by a stochastic geometric model, is independent of both the λ and p parameters, in both the DL and UL directions. In particular, we will analytically identify for such scenario under such model four remarks, for the four combinations of the parameters and directions involved, that defy intuition. We first spotted these remarks in simulation experiments [26], but have since worked to prove them analytically as demonstrated in the sequel. With these remarks identified, it is hoped that the way stochastic geometry is currently applied to wireless communications will be reconsidered.

It should be noted that some of the remarks presented in this article have been alluded to by others, if ever so scantily. For example, the authors of [10] in the context of analyzing DL coverage probability of millimeter-wave cellular networks noted that “coverage does not scale with BS density.” Also, Herath *et al.* [22], in the context of analyzing UL fractional power control (FPC), noted that coverage is “invariant to the density of deployment of BSs when the shadowing is mild and power control is fractional.” Aside from these notes, no one has presented theoretical investigation of these remarks, which was the motive for the present article. It should also be noted that a preliminary version of this article was deposited as a preprint on several renowned repositories, e.g. [27], for maximum exposure and visibility.

The rest of the article is organized as follows. In the method section, we develop the baseline model employed throughout the article as a basis, and analyze it in both DL and UL directions, showing that the coverage probability in both directions is independent of the BS density λ and transmit power p . Numerical results and their explanation are provided in the second section, whereas the last section has the conclusions.

2. METHOD

The key strategy of our method is to construct a SG model for a certain communications system wherein the model fails to deliver adequate results. The inadequacy of the results is presented as four remarks. This strategy is akin to the mathematical strategy of constructing a counter example to invalidate a universal proposition. The principal assumption in the present study, as in most studies of SG modeling of cellular communications systems, is that the BSs are deployed in the Euclidean plane according to a PPP Φ with density λ . We consider cell orthogonal communications, meaning that in each cell only one user equipment (UE) can be active on any time/frequency resource. Accordingly, Figure 1 is a snapshot of the UEs that are active, i.e., communicating with their respective BSs, on the same frequency in all the cells at the same time. Since every BS-UE pair in the Figure operates on the same resource, there is interference which we are going to characterize now. Noise is so dominated by interference that its effect on the received signal can be safely ignored. We incorporate random channel effects by multiplicative RVs, namely G for the signal and G_i for each interferer i . We assume that G and the G_i are independent and identically distributed (iid) random variables (RVs) following an exponential distribution with average 1. In addition, we assume that signals attenuate with distance according to the standard power-law path loss propagation model, with path loss exponent $\alpha > 2$. That is, the average power received at distance r from a transmitter of power p is $pr^{-\alpha}$. Before proceeding further, some important definitions are in order:

- Definition 1 (BS-UE association): BS-UE association is the assignment of a UE to a BS, for establishing a communications channel between the two.
- Definition 2 (Serving BS): once a UE is associated with a BS, the latter is said to be the serving BS of the UE.
- Definition 3 (Typical receiver): the typical receiver is the receiving device (UE or BS) where the SIR is to be assessed. It is always placed at the origin of the Euclidean plane in the SG model, or the origin of the simulation window in a simulation.
- Definition 4 (Tagged transmitter): the tagged transmitter is the transmitting device (UE or BS) associated with the typical receiver.
- Definition 5 (Typical circle): the typical circle is the circle centered at the typical receiver with the tagged

transmitter on its circumference.

- Definition 6 (Interferer): an interferer is a transmitter causing interference at the typical receiver. Thus, it is any transmitter in the cellular network other than the tagged transmitter.
- Definition 7 (Signal to interference ratio (SIR)): the quotient of the signal received at the typical receiver from the tagged transmitter and the sum of all interferences at that receiver.

As per definitions 3 and 4, it is evident that in the DL direction the typical receiver is a UE and the tagged transmitter is a BS, whereas in the UL direction the typical receiver is a BS and the tagged transmitter is a UE. Further, a UE wishing to start a communications session associates with the BS that is closer to it than any other BS in the Euclidean plane (association rule). If we denote the distance between the two elements of a BS-UE pair by R , then R is Rayleigh distributed (since the UE is closer to its associated BS than to any BS in the plane). That is (1).

$$f_R(r) = 2\lambda\pi r e^{-\lambda\pi r^2}, \quad r \geq 0 \quad (1)$$

Referring to Figure 1, the typical receiver resides at the origin, and the tagged transmitter resides on the perimeter of the typical circle of radius R . In the DL model, Figure 1(a), the typical receiver is a UE, and the tagged transmitter is a BS. All the BSs outside the typical circle are interferers to the typical UE. In the UL model, Figure 1(b), the typical receiver is a BS, and the tagged transmitter is a UE. All the UEs, except the tagged UE, are interferers to the typical BS. Along the same line, the notation used throughout the article is provided in Table 1.

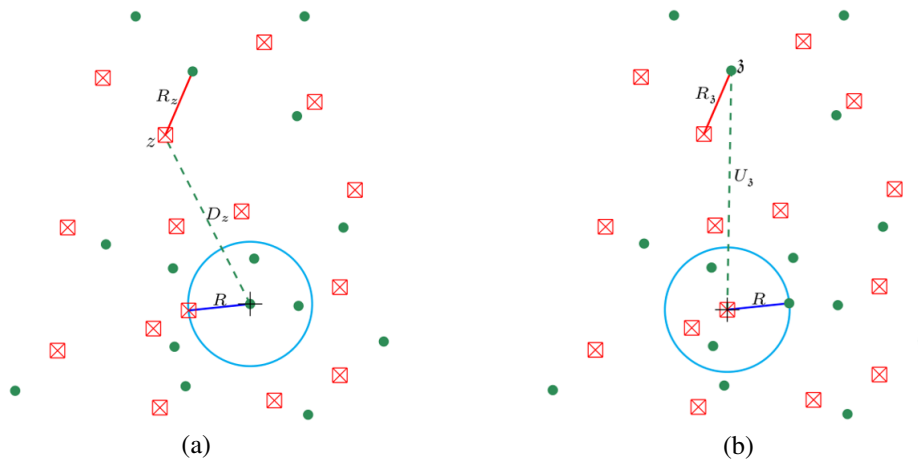


Figure 1. SG models for assessing SIR at a typical receiver (a) DL model and (b) UL model

Table 1. Notation used in the model and simulation

Parameter	Description
Φ	Point process of the BSs (Poisson)
Ψ	Point process of the UEs (not Poisson)
λ	Density of BS (per m^2), i.e. intensity of PPP Φ
α	Path-loss exponent (per m)
SIR	Signal to interference ratio (dB)
ξ	SIR threshold (dB)
G	Rayleigh channel gain of tagged transmitter ($G \sim Exp(1)$)
p	Transmit power (Watts)
p_d	DL coverage probability
p_u	UL coverage probability

2.1. DL model

The key assumptions of the DL system model are:

- Each BS transmits at a fixed power p to the associated UE on a particular time-frequency resource. That is, we consider orthogonal communications within the cell. The consequence of this orthogonality is that each UE sees interference from all the BSs in the plane except its serving BS.

- Random channel effects are incorporated by RV G for the serving BS. And RV G_z for each interfering BS located at point z in the Euclidean plane. We consider Rayleigh fading, and assume that G and the G_z have a common exponential distribution with average 1.

Let I_d be a RV denoting the total DL interference at the typical UE. The interference is due to every BS z in the plane. Except the tagged BS which is denoted by b , as shown in Figure 1(a). Thus it can be seen in (2),

$$I_d = \sum_{z \in \Phi \setminus \{b\}} pG_z D_z^{-\alpha} \tag{2}$$

where D_z is a RV representing the distance between the BS at z and the typical UE. The SIR at the typical UE is thus given by (3).

$$\text{SIR}_{\text{UE}} = \frac{pGR^{-\alpha}}{I_d} \tag{3}$$

The goal now is to derive the DL coverage probability p_d , which is the probability that the SIR at the typical UE exceeds a desired threshold (target) ξ , i.e.,

$$p_d = \mathbb{P}[\text{SIR}_{\text{UE}} > \xi] \tag{4}$$

using (2) and (3) in (4), gives,

$$\begin{aligned} p_d &= \mathbb{P} \left[\frac{pGR^{-\alpha}}{I_d} > \xi \right] \\ &= \mathbb{P} \left[G > \frac{\xi}{p} R^\alpha I_d \right] \\ &\stackrel{(a)}{=} \mathbb{E}_{I_d} \left[\mathbb{P} \left[G > \frac{\xi}{p} R^\alpha I_d \right] \right] \\ &\stackrel{(b)}{=} \mathbb{E}_{I_d} \left[e^{-\frac{\xi}{p} R^\alpha I_d} \right] \\ &= \mathcal{L}_{I_d} \left(\frac{\xi}{p} R^\alpha \right) \end{aligned} \tag{5}$$

where,

$$\mathcal{L}_A(s) = \mathbb{E} [e^{-sA}] = \int_0^\infty e^{-st} f_A(t) dt \tag{6}$$

is the Laplace transform of (the distribution of) any RV A . In (a) we utilized the fact that we can write a probability $\mathbb{P}[A > B]$ as $\mathbb{E}_B[\mathbb{P}[A > B]]$ (or $\mathbb{E}_A[\mathbb{P}[A > B]]$) and in (b) we benefited from the fact that $G \sim \exp(1)$, i.e. $f_G(r) = e^{-r}$. We will now embark on finding an explicit expression for the DL coverage probability p_d in (5) by deconditioning on all the RVs involved.

We start by deconditioning p_d on R , which is Rayleigh distributed, as given by (1), getting:

$$\begin{aligned} p_d &= \int_0^\infty \mathcal{L}_{I_d} \left(\frac{\xi}{p} r^\alpha \right) f_R(r) dr \\ &= 2\tilde{\lambda} \int_0^\infty e^{-\tilde{\lambda} r^2} \mathcal{L}_{I_d} \left(\frac{\xi}{p} r^\alpha \right) r dr, \end{aligned} \tag{7}$$

where $\tilde{\lambda} = \pi\lambda$. The limits of the integral are so set. Since R can range from an arbitrarily small positive real number (to exclude the typical UE) to ∞ , the farthest point to place the tagged UE. We will find the Laplace

transform \mathcal{L}_{I_d} in (7), by using (2) and (6) and then deconditioning on the G_z , to get (8),

$$\begin{aligned}
 \mathcal{L}_{I_d}(s) &= \mathbb{E} \left[e^{-sI_d} \right] \\
 &= \mathbb{E}_{\Phi, G_z} \left[e^{-sp \sum_{z \in \Phi \setminus \{b\}} G_z D_z^{-\alpha}} \right] \\
 &= \mathbb{E}_{\Phi, G_z} \left[\prod_{z \in \Phi \setminus \{b\}} e^{-sp G_z D_z^{-\alpha}} \right] \\
 &\stackrel{(a)}{=} \mathbb{E}_{\Phi} \left[\prod_{z \in \Phi \setminus \{b\}} \mathbb{E}_{G_z} \left[e^{-sp G_z D_z^{-\alpha}} \right] \right] \\
 &\stackrel{(b)}{=} \mathbb{E}_{\Phi} \left[\prod_{z \in \Phi \setminus \{b\}} \mathcal{L}_{G_z}(sp D_z^{-\alpha}) \right] \tag{8}
 \end{aligned}$$

in (a) we exploited the independence of the G_z . In (b) we used the definition (6) of the Laplace transform.

Next, we decondition on Φ by invoking the PGFL for the point process (since each D_z is distributed differently for each $z \in \Phi$) defined as (9),

$$\mathbb{E}_{\Phi} \left[\prod_{z \in \Phi} f(z) \right] = \exp \left(-\lambda \int_{\mathbb{R}^2 \setminus D(o,r)} (1 - f(\chi)) \right) \tag{9}$$

where $D(o, r)$ is a disk of radius r centered at the origin, forming an exclusion zone. Applying (9) in (8), we get (10),

$$\mathcal{L}_{I_d}(s) = \exp \left(-\lambda \int_{\mathbb{R}^2 \setminus D(o,r)} (1 - \mathcal{L}_{G_z}(sp \chi^{-\alpha})) \right) \tag{10}$$

Using polar coordinates for the integral, with the interferer located at $(x, \theta) \in \mathbb{R}^2$. Using also the fact that $G_z \sim \exp(1)$. i.e., $f_{G_z}(t) = e^{-t}$ and $\mathcal{L}_{G_z}(s) = 1/(1+s)$, we get (11),

$$\begin{aligned}
 \mathcal{L}_{I_d}(s) &= \exp \left(-\lambda \int_r^\infty \int_0^{2\pi} \left(1 - \frac{1}{1 + spx^{-\alpha}} \right) d\theta dx \right) \\
 &= \exp \left(-2\tilde{\lambda} \int_r^\infty \frac{spx^{-\alpha}}{1 + spx^{-\alpha}} x dx \right) \tag{11}
 \end{aligned}$$

note that we integrate with respect to x from r to ∞ since the interference emanates from outside the exclusion zone $D(o, r)$.

To find the transform $\mathcal{L}_{I_d}(\frac{\xi}{p} r^\alpha)$ needed in (7), we update the argument in (11), getting (12).

$$\begin{aligned}
 \mathcal{L}_{I_d}\left(\frac{\xi}{p} r^\alpha\right) &= \exp \left(-2\tilde{\lambda} \int_r^\infty \left(\frac{\xi r^\alpha p x^{-\alpha}}{1 + \xi r^\alpha p x^{-\alpha}} \right) x dx \right) \\
 &= \exp \left(-2\tilde{\lambda} \int_r^\infty \frac{\xi \left(\frac{r}{x}\right)^\alpha}{1 + \xi \left(\frac{r}{x}\right)^\alpha} x dx \right) \\
 &= \exp \left(-2\tilde{\lambda} \int_r^\infty \frac{\xi}{\left(\frac{x}{r}\right)^\alpha + \xi} x dx \right) \tag{12}
 \end{aligned}$$

Remark 1: We note from (12) that the BS power p has disappeared. This indicates that the DL coverage probability, obtained by substituting (12) in (7), is independent of BS power. This is counter intuitive, as in practice cell phone carriers increase BS power to boost coverage and vice versa.

Now, use in (12) the substitution $u = (x/r)^2 \xi^{-\frac{2}{\alpha}}$, which implies $(x/r)^2 = u \xi^{\frac{2}{\alpha}}$, which means $(x/r) = u^{\frac{1}{2}} \xi^{\frac{1}{\alpha}}$, giving $(x/r)^\alpha = u^{\alpha/2} \xi$. Then take the derivative of u with respect to x to get $du =$

$2(x/r)\frac{1}{r}\xi^{-\frac{2}{\alpha}}dx$ which gives $du = 2xdx/(r^2\xi^{\frac{2}{\alpha}})$, i.e. $xdx = \frac{1}{2}r^2\xi^{\frac{2}{\alpha}}du$. Finally, at $x = r$, then $u = \xi^{-\frac{2}{\alpha}}$, and at $x = \infty$, then $u = \infty$. With this in mind, (12) becomes,

$$\begin{aligned} \mathcal{L}_{I_d}\left(\frac{\xi}{p}r^\alpha\right) &= \exp\left(-2\tilde{\lambda}\int_{\xi^{-\frac{2}{\alpha}}}^{\infty}\frac{\xi}{\left(u^{\frac{1}{2}}\xi^{\frac{1}{\alpha}}\right)^\alpha + \xi^2}\frac{1}{2}r^2\xi^{\frac{2}{\alpha}}du\right) \\ &= \exp\left(-\tilde{\lambda}r^2\xi^{\frac{2}{\alpha}}\int_{\xi^{-\frac{2}{\alpha}}}^{\infty}\frac{\xi}{\left(u^{\frac{1}{2}}\xi^{\frac{1}{\alpha}}\right)^\alpha + \xi^2}du\right) \\ &= \exp\left(-\tilde{\lambda}r^2\xi^{\frac{2}{\alpha}}\int_{\xi^{-\frac{2}{\alpha}}}^{\infty}\frac{\xi}{u^{\frac{\alpha}{2}}\xi + \xi}du\right) \\ &= \exp\left(-\tilde{\lambda}r^2\sqrt[\kappa]{\xi}\int_{\frac{1}{\sqrt[\kappa]{\xi}}}^{\infty}\frac{1}{1+u^\kappa}du\right) \end{aligned}$$

where $\kappa = \alpha/2$. Substituting this in (7), we get for the DL coverage probability the expression.

$$p_d = 2\tilde{\lambda}\int_0^\infty e^{-\tilde{\lambda}r^2}e^{-\tilde{\lambda}r^2\sqrt[\kappa]{\xi}\int_{\frac{1}{\sqrt[\kappa]{\xi}}}^\infty\frac{1}{1+u^\kappa}du}rdr. \tag{13}$$

Although the BS density λ appears in (13), deceiving some researchers, we will show next, via two changes of variables, that it is superfluous. First, use the substitution $x = r^2$ in (13) to get,

$$p_d = \tilde{\lambda}\int_0^\infty e^{-\tilde{\lambda}x}\left(1+\sqrt[\kappa]{\xi}\int_{\frac{1}{\sqrt[\kappa]{\xi}}}^\infty\frac{1}{1+u^\kappa}du\right)dx$$

second, use the substitution $z = \tilde{\lambda}x$, to get,

$$\begin{aligned} p_d &= \int_0^\infty e^{-z}\left(1+\sqrt[\kappa]{\xi}\int_{\frac{1}{\sqrt[\kappa]{\xi}}}^\infty\frac{1}{1+u^\kappa}du\right)dz \\ &= \frac{1}{1+\sqrt[\kappa]{\xi}\int_{\frac{1}{\sqrt[\kappa]{\xi}}}^\infty\frac{1}{1+u^\kappa}du} \end{aligned} \tag{14}$$

where λ has disappeared.

Remark 2: We can see from (14) that the BS density λ has disappeared. This indicates that the DL coverage probability is independent of the BS density. This is counter intuitive, as in practice cell phone carriers increase BS density if they want to boost coverage and vice versa.

2.2. UL model

In the UL direction, the interference at the typical BS is basically the sum of the received transmissions from all the UEs (including those inside the typical circle), except the tagged UE. Referring to Figure 1(b), we assume that the BSs constitute a PPP Φ of density λ , and the UEs constitute another point process Ψ of the same density (as each UE is associated with one and only one BS, and vice versa). Referring to Figure 1(b), for each UE $\mathfrak{z} \in \Psi$, we denote the distance to its serving BS by $R_{\mathfrak{z}}$ and denote the distance to the typical BS by $U_{\mathfrak{z}}$. To distinguish it from all other distances, we denote by R the distance between the tagged UE and the typical BS. As can be seen in Figure 1(b), RV $R_{\mathfrak{z}}$ is upper bounded by $U_{\mathfrak{z}}$ (otherwise the UE at \mathfrak{z} would associate with the typical BS.) Also, both R and $R_{\mathfrak{z}}$ are Rayleigh distributed, as per (1), as they express associations based on shortest distances.

On the other hand, we will assume FPC, where each UE adjusts its power level based on its current distance to the serving BS [7]. If the distance between a UE and its serving BS is $R_{\mathfrak{z}}$ and the FPC factor is $\epsilon \in [0, 1]$, then the transmit power p of the UE is amplified by $R_{\mathfrak{z}}^{\epsilon\alpha}$ to offset the path loss, $R_{\mathfrak{z}}^{-\alpha}$. If $\epsilon = 0$, there is no offset, meaning the transmit power is invariant to distance, and if it is 1 there is complete channel inversion.

That said, the interference at the typical BS in the UL model is (15),

$$I_u = \sum_{\mathfrak{z} \in \Psi \setminus \{u\}} pG_{\mathfrak{z}}R_{\mathfrak{z}}^{\alpha\epsilon}U_{\mathfrak{z}}^{-\alpha}, \quad (15)$$

where u denotes the tagged UE. Combining FPC and power loss, the net power reaching the BS from the UE is $pGR_{\mathfrak{z}}^{-\alpha(1-\epsilon)}$. Also the SIR at the typical BS is (16).

$$\text{SIR}_{\text{BS}} = \frac{pGR^{-\alpha(1-\epsilon)}}{I_u} \quad (16)$$

The goal now is to derive the UL coverage probability p_u , which is the probability that the SIR at the typical BS exceeds a desired threshold ξ , i.e.,

$$p_u = \mathbb{P}[\text{SIR}_{\text{BS}} > \xi] \quad (17)$$

using (15), (16) and (17), the UL coverage probability is (18),

$$\begin{aligned} p_u &= \mathbb{E} \left[\mathbb{P} \left[\frac{pGR^{-\alpha(1-\epsilon)}}{I_u} > \xi \right] \right] \\ &= \mathbb{E} \left[\mathbb{P} \left[G > \xi p^{-1} R^{\alpha(1-\epsilon)} I_u \right] \right] \\ &\stackrel{(a)}{=} \mathbb{E} \left[e^{-\xi p^{-1} I_u R^{\alpha(1-\epsilon)}} \right] \\ &= \mathcal{L}_{I_u}(\xi p^{-1} R^{\alpha(1-\epsilon)}) \end{aligned} \quad (18)$$

where \mathcal{L}_{I_u} is the Laplace transform of the distribution of I_u . In (a), we used the fact that $G \sim \exp(1)$, i.e. $f_G(x) = e^{-x}$, which implies that $\mathbb{P}[G > x] = e^{-x}$.

Now, we decondition p_u in (18) on R , getting (19).

$$\begin{aligned} p_u &= \int_0^\infty \mathcal{L}_{I_u}(\xi p^{-1} r^{\alpha(1-\epsilon)}) f_R(r) dr \\ &= \int_0^\infty 2\tilde{\lambda} r e^{-\tilde{\lambda} r^2} \mathcal{L}_{I_u}(\xi p^{-1} r^{\alpha(1-\epsilon)}) dr. \end{aligned} \quad (19)$$

Note that we integrate from just outside the origin, to skip the typical BS, to ∞ where the closest UE can possibly exist.

Next, we will embark on finding for (19) the transform $\mathcal{L}_{I_u}(s) = \mathbb{E}[e^{-sI_u}]$. Using (15), we get (20),

$$\begin{aligned} \mathcal{L}_{I_u}(s) &= \mathbb{E} \left[e^{-s \sum_{\mathfrak{z} \in \Psi} pG_{\mathfrak{z}}R_{\mathfrak{z}}^{\alpha\epsilon}U_{\mathfrak{z}}^{-\alpha}} \right] \\ &= \mathbb{E} \left[\prod_{\mathfrak{z} \in \Psi} e^{-spG_{\mathfrak{z}}R_{\mathfrak{z}}^{\alpha\epsilon}U_{\mathfrak{z}}^{-\alpha}} \right] \\ &= \mathbb{E}_{\Psi, R_{\mathfrak{z}}, G_{\mathfrak{z}}} \left[\prod_{\mathfrak{z} \in \Psi} e^{-spG_{\mathfrak{z}}R_{\mathfrak{z}}^{\alpha\epsilon}U_{\mathfrak{z}}^{-\alpha}} \right], \end{aligned} \quad (20)$$

where we have written Ψ instead of $\Psi \setminus \{u\}$ just for simplicity. In (20), for each point $\mathfrak{z} \in \Psi$ there correspond three RVs: $G_{\mathfrak{z}}, R_{\mathfrak{z}}, U_{\mathfrak{z}}$. The $G_{\mathfrak{z}}$ are independent of both $R_{\mathfrak{z}}$ and $U_{\mathfrak{z}}$, whereas $U_{\mathfrak{z}}$ and $R_{\mathfrak{z}}$ are dependent, as $R_{\mathfrak{z}} < U_{\mathfrak{z}}$ must hold, since if $U_{\mathfrak{z}} < R_{\mathfrak{z}}$ the interfering UE at \mathfrak{z} would associate with the typical BS at the origin. That is, $\mathbb{P}[R_{\mathfrak{z}} < x | U_{\mathfrak{z}} = x] = 1$.

Now, we decondition $\mathcal{L}_{I_u}(s)$ on G_3 , getting:

$$\begin{aligned} \mathcal{L}_{I_u}(s) &\stackrel{(a)}{=} \mathbb{E}_{\Psi, R_3} \left[\prod_{3 \in \Psi} \mathbb{E}_{G_3} \left[e^{-spG_3 R_3^{\alpha\epsilon} U_3^{-\alpha}} \right] \right] \\ &\stackrel{(b)}{=} \mathbb{E}_{\Psi, R_3} \left[\prod_{3 \in \Psi} \int_0^\infty e^{-(1+spR_3^{\alpha\epsilon} U_3^{-\alpha})x} dx \right] \\ &= \mathbb{E}_{\Psi, R_3} \left[\prod_{3 \in \Psi} \frac{1}{1 + spR_3^{\alpha\epsilon} U_3^{-\alpha}} \right] \end{aligned} \tag{21}$$

in (a) we used the fact that the G_3 are iid and in (b) we used the fact that $f_{G_3}(x) = e^{-x}$.

Next, we consider the expectation with respect to Ψ , in order to decondition on U_3 , the distance between every point $3 \in \Psi$ and the origin. We will use for this expectation a PGFL, since U_3 is distributed differently for each 3 . However, Ψ is not poisson, as its points are not randomly and independently distributed in the Euclidean plane, as was the case with Φ , but are rather *satellites* to the points of Φ . Consequently, we cannot in principle apply a PGFL, as it assumes a PPP, for this deconditioning. To get around this difficulty, we will employ an approximation.

From the assumptions, each UE is situated randomly around its serving BS. That is, each point of Ψ is positioned randomly around a point of Φ . Thus, we can approximate the locations of the points of Ψ by the locations of the points of Φ , when characterizing the UL interference caused by the UEs as follows. When characterizing the interference caused by a UE, we will employ for its distance to the typical BS the RV D_z , rather than the RV U_3 . That is, we will consider each UE to be at a point $z \in \Phi$, emitting power $pR_3^{\alpha\epsilon}$, to cause interference at the typical BS, at distance D_z . Accordingly,

$$\mathbb{E}_{\Psi} \left[\prod_{3 \in \Psi} f(3) \right] \approx \mathbb{E}_{\Phi} \left[\prod_{z \in \Phi} f(z) \right]$$

where the RHS is as given by (9). Using this approximation in (21) yields.

$$\mathcal{L}_{I_u}(s) = \mathbb{E}_{R_3} \left[\mathbb{E}_{\Phi} \left[\prod_{z \in \Phi} \frac{1}{1 + spR_3^{\alpha\epsilon} D_z^{-\alpha}} \right] \right]$$

Recall that D_z , instead of the real distance U_3 , is now considered (by our approximation) the distance between the UE at 3 and the origin. Applying the PGFL \mathbb{E}_{Φ} , using polar coordinates. Also substituting for the angle integral by 2π , yield,

$$\mathcal{L}_{I_u}(s) = e^{-2\tilde{\lambda} \int_0^\infty \left(\mathbb{E}_{R_3} \left[\frac{1}{1+(sp)^{-1} R_3^{-\alpha\epsilon} x^\alpha} \right] \right) x dx}$$

we will decondition next on the R_3 , which are independent and identically Rayleigh distributed as per (1) Note, however, that the two RVs $D_z^{-\alpha}$ and R_3 are dependent since $R_3 < D_z$ must hold. This means that the upper limit of the deconditioning integral below should be the x in the above integral. Thus,

$$\begin{aligned} \mathcal{L}_{I_u}(s) &= e^{-2\tilde{\lambda} \int_0^\infty \left(\int_0^x \frac{1}{1+(sp)^{-1} y^{-\alpha\epsilon} x^\alpha} f_{R_3}(y) dy \right) x dx} \\ &= e^{-2\tilde{\lambda} \int_0^\infty \left(\int_0^x \frac{2\lambda\pi y e^{-\lambda\pi y^2}}{1+(sp)^{-1} y^{-\alpha\epsilon} x^\alpha} dy \right) x dx} \\ &= e^{-2\tilde{\lambda}^2 \int_0^\infty x \int_0^{x^2} \frac{e^{-\tilde{\lambda}u}}{1+(sp)^{-1} u^{-\alpha\epsilon/2} x^\alpha} dudx} \end{aligned} \tag{22}$$

from (22), we can write,

$$\begin{aligned} \mathcal{L}_{I_u}(\xi p^{-1} r^{\alpha(1-\epsilon)}) &= e^{-2\tilde{\lambda}^2 \int_0^\infty x \int_0^{x^2} \frac{e^{-\tilde{\lambda}u}}{1+(\xi p^{-1} r^{\alpha(1-\epsilon)})^{-1} u^{-\alpha\epsilon/2} x^\alpha} dudx} \\ &= e^{-2\tilde{\lambda}^2 \int_0^\infty x \int_0^{x^2} \frac{\xi r^{\alpha(1-\epsilon)} e^{-\tilde{\lambda}u}}{\xi r^{\alpha(1-\epsilon)} + u^{-\alpha\epsilon/2} x^\alpha} dudx} \end{aligned} \tag{23}$$

Remark 3: We note from (23) that the UE power p has disappeared. This indicates that the UL coverage probability, obtained by substituting (23) in (19), is independent of UE power. This is counter intuitive, as in practice cell phone manufacturers increase UE power if they want to boost coverage and vice versa.

Using (23) in (19), we get (24).

$$p_u = 2\tilde{\lambda} \int_0^\infty r e^{-\tilde{\lambda}r^2} e^{-2\tilde{\lambda}^2 \xi r^{2\kappa(1-\epsilon)}} \int_0^\infty x \int_0^{x^2} \frac{e^{-\tilde{\lambda}u}}{\xi r^{2\kappa(1-\epsilon)} + u^{-\epsilon\kappa} x^{2\kappa}} du dx dr \quad (24)$$

Although the BS density λ appears in (25), we will show below, via a sequence of variable changes, that it is superfluous.

Start by using the substitution $v = r^2$ in (24), to get.

$$p_u = \tilde{\lambda} \int_0^\infty e^{-\tilde{\lambda}v} e^{-2\tilde{\lambda}^2 \xi v^{\kappa(1-\epsilon)}} \int_0^\infty x \int_0^{x^2} \frac{e^{-\tilde{\lambda}u}}{\xi v^{\kappa(1-\epsilon)} + u^{-\epsilon\kappa} x^{2\kappa}} du dx dv$$

Use $y = x^2$ to get,

$$p_u = \tilde{\lambda} \int_0^\infty e^{-\tilde{\lambda}v} e^{-\tilde{\lambda}^2 \xi v^{\kappa(1-\epsilon)}} \int_0^\infty \int_0^y \frac{e^{-\tilde{\lambda}u}}{\xi v^{\kappa(1-\epsilon)} + u^{-\epsilon\kappa} y^\kappa} du dy dv$$

Use $x = \tilde{\lambda}u$ to get,

$$p_u = \tilde{\lambda} \int_0^\infty e^{-\tilde{\lambda}v} e^{-\tilde{\lambda}^2 \xi v^{\kappa(1-\epsilon)}} \int_0^\infty \int_0^{\tilde{\lambda}y} \frac{e^{-x}}{\xi v^{\kappa(1-\epsilon)} + \left(\frac{x}{\tilde{\lambda}}\right)^{-\epsilon\kappa} y^\kappa} dx dy dv$$

Use $z = \tilde{\lambda}v$ to get,

$$p_u = \int_0^\infty e^{-z} e^{-\tilde{\lambda} \xi z^{\kappa(1-\epsilon)}} \int_0^\infty \int_0^{\tilde{\lambda}y} \frac{e^{-x}}{\xi z^{\kappa(1-\epsilon)} + x^{-\epsilon\kappa} \left(\frac{\tilde{\lambda}y}{z}\right)^\kappa} dx dy dz$$

Finally, use $u = \tilde{\lambda}y$ to get,

$$p_u = \int_0^\infty e^{-z} \left(1 + \xi z^{\kappa(1-\epsilon)-1} \int_0^\infty \int_0^u \frac{e^{-x}}{\xi z^{\kappa(1-\epsilon)} + x^{-\epsilon\kappa} u^\kappa} dx du\right) dz \quad (25)$$

where λ has disappeared, proving the theorem.

Remark 4: We note from (25) that the UL coverage probability is independent of BS density. Similar to Remarks 1, 2, and 3, this behavior is counter intuitive. This is because in practice cell phone carriers increase BS density to boost coverage and vice versa.

3. RESULTS AND DISCUSSION

In this section, we will investigate the coverage probability for an example interference-limited cellular system with the assumptions stated at the beginning of the article. The aim is to validate the findings of the article, namely, the four remarks above. Specifically, we will evaluate the coverage probability, in both the DL and UL directions, for two values of the path loss exponent α (4 and 6) and, in the case of UL, three values of the power control factor ϵ (0, 0.5 and 1) using both the analytical results, derived above, and Monte Carlo simulation, used for validation.

For the simulation, we developed our own simulator using the MATLAB language, and employed it for both the DL and UL communications. For each simulation run, we would randomly spread a random number of BSs over the simulation area, a square of side 3,000 m. The number of BSs is Poisson distributed with some average, λ . Then we would allow the devices to communicate at some power p . Finally, we evaluate the coverage probability at the receiver, which is the UE in the case of DL and BS in the case of UL, by estimating the number of devices whose reception exceeds the intended threshold ξ . From our experimentation, we found that 10,000 simulation runs are enough to reach convergence; more runs would be wasteful.

In the four graphs below, we sketch the coverage probability against the SIR threshold, ξ . The line represents the analytical results, namely (14) and (25), while the bullets represent the simulation results. We can see that both types of results match almost identically, confirming our analytical derivations. The first two graphs are for DL and the second two are for UL. We can first see, that regardless of direction, DL or UL, the coverage probability decreases (non-linearly) as the threshold increases which is logical. As the threshold is the reference for evaluating the coverage, the higher the threshold the lower the probability of exceeding it. In Figure 2, we have a sketch of the DL coverage probability, p_d , against SIR threshold ξ , when the path loss exponent $\alpha=4$ ($\kappa=2$). As mentioned earlier, the coverage probability decreases, non-linearly, with the SIR threshold, ξ . For $\alpha=6$, Figure 3, we still have the same general pattern as for $\alpha = 4$, but the coverage probability is obviously higher. Specifically, raising α results in raising the coverage probability, for the same ξ . The increase of the coverage probability with α is more noticeable for positive ξ .

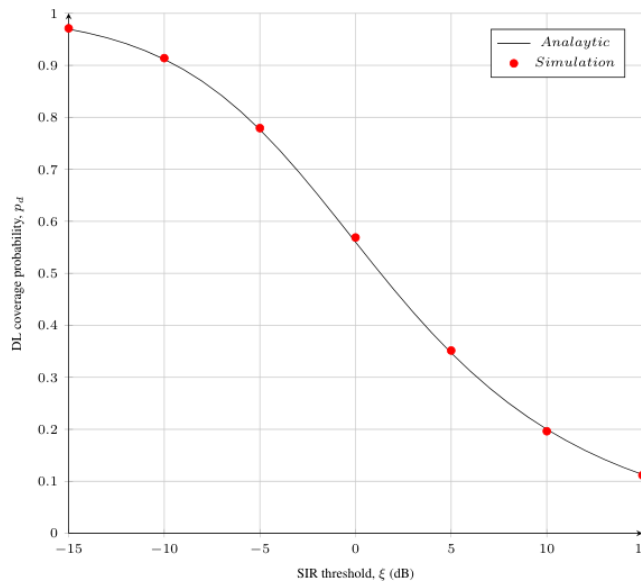


Figure 2. DL coverage probability, p_d , against SIR threshold ξ when the path loss exponent $\alpha = 4$ ($\kappa = 2$)

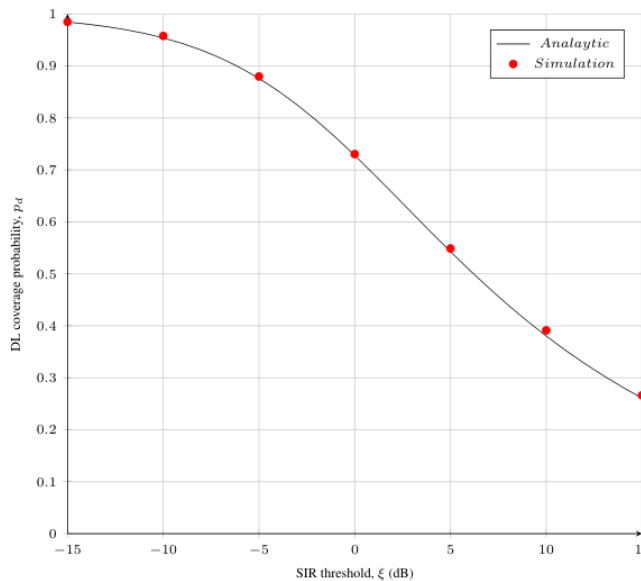


Figure 3. DL coverage probability, p_d , against SIR threshold ξ when the path loss exponent $\alpha = 6$ ($\kappa = 3$)

In Figure 4, we sketch the UL coverage probability, p_u , against SIR threshold, ξ , when the path loss exponent $\alpha = 4$ ($\kappa = 2$), for three values of the power control factor, $\epsilon \in 0, 0.5, 1$. We can see that the effect of the power control factor varies according to the value of ξ . Specifically, a higher ϵ provides better coverage at low ξ , but worse coverage at high ξ . The same comments apply when $\alpha = 6$, in Figure 5. As can be seen, the coverage probability increases as the path loss exponent increases, especially for positive ξ , with all other variables kept the same.

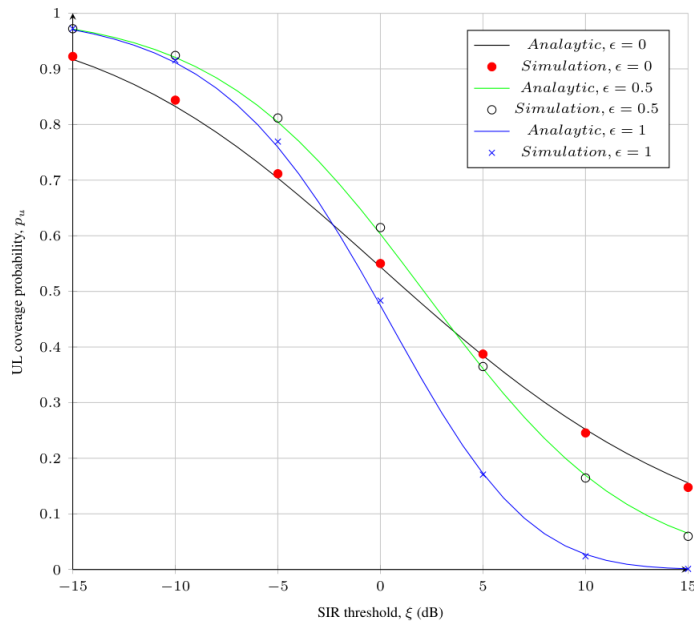


Figure 4. UL coverage probability, p_u , against SIR threshold ξ when the path loss exponent $\alpha = 4$ ($\kappa = 2$), for three power control values $\epsilon \in 0, 0.5, 1$

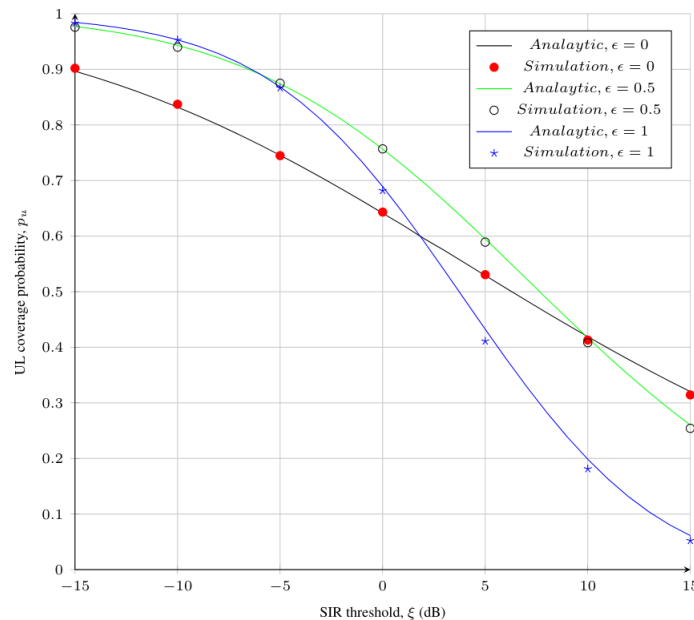


Figure 5. UL coverage probability, p_u , against SIR threshold ξ when the path loss exponent $\alpha = 6$ ($\kappa = 3$), for three power control values $\epsilon \in 0, 0.5, 1$

4. CONCLUSION

In this article we have presented four counter intuitive remarks concerning a SG model of a particular cellular setup, thus pointing to a glitch in the way SG is currently applied to model communications systems. Namely, we have proved that under some assumptions, the coverage probability of a particular cellular system, in either DL and UL, is invariant to both BS density λ and transmit power p something that obviously defies intuition. We do not intend by this revelation to invalidate SG as a modeling tool of communications systems. Needless to say, SG has shown undeniable success in this regard, as has been demonstrated by countless studies over the past two decades. Rather, we intend to call for efforts to find out the cause of the revealed anomaly and propose modeling measures that can avoid it. Also, we intend to alert SG researchers to scrutinize their results deeply enough for such anomalies, as it is typically the case that these results are so cumbersome that superfluous parameters within them can go deceitfully undetected.





REFERENCES

- [1] E. Noma-Osaghae, S. Misra, and M. Koyuncu, "Optimizing the stochastic deployment of small base stations in an interleave division multiple access-based heterogeneous cellular networks," *International Journal of Communication Systems*, vol. 35, no. 12, 2022, doi: 10.1002/dac.5204.
- [2] S. Ali, M. I. Aslam, I. Ahmed, and A. Khawaja, "Uplink performance of narrowband internet-of-things devices in downlink–uplink decoupled-based heterogeneous networks," *Iranian Journal of Science and Technology - Transactions of Electrical Engineering*, vol. 47, no. 2, pp. 385–399, 2023, doi: 10.1007/s40998-022-00570-w.
- [3] F. Xu, Y. Hu, Z. Hu, and H. Cao, "Coverage probability analysis for device-to-device communication underlying cellular networks," *Electronics (Switzerland)*, vol. 11, no. 3, p. 464, 2022, doi: 10.3390/electronics11030464.
- [4] H. Mariam, I. Ahmed, S. Ali, M. I. Aslam, and I. U. Rehman, "Performance of millimeter wave dense cellular network using stretched exponential path loss model," *Electronics (Switzerland)*, vol. 11, no. 24, p. 4226, 2022, doi: 10.3390/electronics11244226.
- [5] C. H. Liu, Y. H. Shen, and C. H. Lee, "Energy-efficient activation and uplink transmission for cellular IoT," *IEEE Internet of Things Journal*, vol. 7, no. 2, pp. 906–921, 2020, doi: 10.1109/JIOT.2019.2946331.
- [6] Q. Liu and Z. Zhang, "The analysis of coverage probability, ASE and EE in heterogeneous ultra-dense networks with power control," *Digital Communications and Networks*, vol. 6, no. 4, pp. 524–533, 2020, doi: 10.1016/j.dcan.2020.02.002.
- [7] N. Kouzayha, H. Elsayy, H. Dahrouj, and T. Y. Al-Naffouri, "Meta distribution of downlink SIR for binomial point processes," *IEEE Wireless Communications Letters*, vol. 10, no. 7, pp. 1557–1561, 2021, doi: 10.1109/LWC.2021.3074399.
- [8] H. ElSawy, A. Sultan-Salem, M. S. Alouini, and M. Z. Win, "Modeling and analysis of cellular networks using stochastic geometry: a tutorial," *IEEE Communications Surveys and Tutorials*, vol. 19, no. 1, pp. 167–203, 2017, doi: 10.1109/COMST.2016.2624939.
- [9] T. Bai and R. W. Heath, "Coverage and rate analysis for millimeter-wave cellular networks," *IEEE Transactions on Wireless Communications*, vol. 14, no. 2, pp. 1100–1114, 2015, doi: 10.1109/TWC.2014.2364267.
- [10] J. Chen and C. Yuan, "Coverage probability and average rate of downlink user-centric wireless cellular networks with composite $\kappa - \mu$ shadowed and lognormal shadowed fading," *IET Communications*, vol. 13, no. 17, pp. 2805–2813, 2019, doi: 10.1049/iet-com.2019.0220.
- [11] Q. Liu, J. Y. Baudais, and P. Mary, "A tractable coverage analysis in dynamic downlink cellular networks," in *IEEE Workshop on Signal Processing Advances in Wireless Communications, SPAWC, 2020*, vol. 2020-May, pp. 1–5, doi: 10.1109/SPAWC48557.2020.9154321., doi: 10.1109/SPAWC48557.2020.9154321.
- [12] M. A. Ouamri, M. E. Oteşteanu, A. Isar, and M. Azni, "Coverage, Handoff and cost optimization for 5G heterogeneous network," *Physical Communication*, vol. 39, no. 5, p. 101037, 2020, doi: 10.1016/j.phycom.2020.101037.
- [13] J. Lei, H. Chen, and F. Zhao, "Stochastic geometry analysis of downlink spectral and energy efficiency in ultradense heterogeneous cellular networks," *Mobile Information Systems*, vol. 2018, no. 1684128, 2018, doi: 10.1155/2018/1684128.
- [14] M. M. Fadoul, "Rate and coverage analysis in multi-tier heterogeneous network using stochastic geometry approach," *Ad Hoc Networks*, vol. 98, no. 102038, 2020, doi: 10.1016/j.adhoc.2019.102038.
- [15] Y. Gao, S. Yang, S. Wu, M. Wang, and X. Song, "Coverage probability analysis for mmwave communication network with absf-based interference management by stochastic geometry," *IEEE Access*, vol. 7, pp. 133572–133582, 2019, doi: 10.1109/ACCESS.2019.2940537.
- [16] S. Ali, M. I. Aslam, and I. Ahmed, "Uplink coverage probability and spectral efficiency for downlink uplink decoupled dense heterogeneous cellular network using multi-slope path loss model," *Telecommunication Systems*, vol. 72, no. 4, pp. 505–516, 2019, doi: 10.1007/s11235-019-00587-3.
- [17] J. G. Andrews, A. K. Gupta, and H. S. Dhillon, "A primer on cellular network analysis using stochastic geometry," *ArXiv*, 2016, doi: 10.48550/arXiv.1604.03183.
- [18] A. M. Kundu, R. Pal, M. Kumar, and S. T V, "Uplink and downlink performance bounds for full duplex cellular networks," in *2020 IEEE International Black Sea Conference on Communications and Networking, BlackSeaCom 2020*, 2020, pp. 1–6, doi: 10.1109/BlackSeaCom48709.2020.9235024., doi: 10.1109/BlackSeaCom48709.2020.9235024.
- [19] E. Sadeghabadi, S. M. Azimi-Abarghouyi, B. Makki, M. Nasiri-Kenari, and T. Svensson, "Asynchronous downlink massive MIMO networks: a stochastic geometry approach," *IEEE Transactions on Wireless Communications*, vol. 19, no. 1, pp. 579–594, 2020, doi: 10.1109/TWC.2019.2946824.
- [20] X. Wang and M. C. Gursoy, "Coverage analysis for energy-harvesting UAV-assisted mmWave cellular networks," *IEEE Journal on Selected Areas in Communications*, vol. 37, no. 12, pp. 2832–2850, 2019, doi: 10.1109/JSAC.2019.2947929.
- [21] M. S. Haroon, F. Muhammad, Z. H. Abbas, G. Abbas, N. Ahmed, and S. Kim, "Proactive uplink interference management for nonuniform heterogeneous cellular networks," *IEEE Access*, vol. 8, pp. 55501–55512, 2020, doi: 10.1109/ACCESS.2020.2981631.





- [22] P. Herath, C. Tellambura, and W. A. Krzymień, "Coverage probability analysis of three uplink power control schemes: Stochastic geometry approach," *Eurasip Journal on Wireless Communications and Networking*, vol. 2018, no. 1, p. 141, 2018, doi: 10.1186/s13638-018-1120-7.
- [23] N. Kouzayha, Z. Dawy, J. G. Andrews, and H. ElSawy, "Joint Downlink/Uplink RF wake-up solution for IoT over cellular networks," *IEEE Transactions on Wireless Communications*, vol. 17, no. 3, pp. 1574–1588, 2018, doi: 10.1109/TWC.2017.2781696.
- [24] H. Mariam, I. Ahmed, and M. I. Aslam, "Coverage probability of uplink millimeter wave cellular network with non-homogeneous interferers' point process," *Physical Communication*, vol. 45, p. 101274, 2021, doi: 10.1016/j.phycom.2021.101274.
- [25] X. Jia, Q. Fan, W. Xu, and L. Yang, "Cross-tier dual-connectivity designs of three-tier hetnets with decoupled uplink/downlink and global coverage performance evaluation," *IEEE Access*, vol. 7, pp. 16816–16836, 2019, doi: 10.1109/ACCESS.2019.2895389.
- [26] H. Nassar, G. Taher, and E. El-Hady, "Stochastic geometric modelling and simulation of cellular systems for coverage probability characterization," *ArXiv*, doi: 10.48550/arXiv.2109.14063.
- [27] H. Nassar, G. Taher, and E.-S. El-Hady, "Cellular coverage probability is independent of base station density under stochastic geometric models," *SSRN Electronic Journal*, 2021, doi: 10.2139/ssrn.3936557.

BIOGRAPHIES OF AUTHORS







Hamed Nassar     received the B.Sc. degree in electrical engineering from Ain Shams University, Egypt, in May 1979, and the M.Sc. degree in electrical engineering and the Ph.D. degree in computer engineering from the New Jersey Institute of Technology, USA, in May 1985 and May 1989, respectively. He has been a full professor in the Department of Computer Science, Suez Canal University, Egypt, since 2004. Besides Egypt, he has taught computer science and engineering courses in USA, Lebanon and Saudi Arabia. Dr. Nassar has published numerous articles in international journals and conferences. His research interests include mathematical modelling of computer and communications systems, cloud computing and machine learning. He can be contacted at email: nassar@ci.suez.edu.eg.



Gehad Mohamed Taher     is Teacher Assistance in the Computer Science Department, Suez Canal University, Egypt. She received her B.Sc. and M.Sc. in Computer Science from the same University in 2003 and 2015 respectively. Her research interests include IoT, wireless networks, modeling, and simulation. She can be contacted at email: gehad.taher@ci.suez.edu.eg.



El Sayed El Hady     is Assistant Professor in the Basic Science Department, Suez Canal University, Egypt. He received his B.Sc. and M.Sc. in Mathematics from the same University in 2004 and 2010 respectively. He received his Ph.D. in Mathematics from Innsbruck University, Austria in 2016. His research interests include mathematical modeling, functional equations, and stability of (functional, differential, fractional differential) equations. He can be contacted at email: elsayed_elhady@ci.suez.edu.eg.